

The miR-200 family and miR-205 regulate epithelial to mesenchymal transition by targeting ZEB1 and SIP1

Philip A. Gregory^{1,4}, Andrew G. Bert¹, Emily L. Paterson¹, Simon C. Barry², Anna Tsykin¹, Gelareh Farshid³, Mathew A. Vadas^{1,4,6}, Yeeseim Khew-Goodall^{1,5,7} and Gregory J. Goodall^{1,4,7,8}

Epithelial to mesenchymal transition (EMT) facilitates tissue remodelling during embryonic development and is viewed as an essential early step in tumour metastasis. We found that all five members of the microRNA-200 family (miR-200a, miR-200b, miR-200c, miR-141 and miR-429) and miR-205 were markedly downregulated in cells that had undergone EMT in response to transforming growth factor (TGF)- β or to ectopic expression of the protein tyrosine phosphatase Pez. Enforced expression of the miR-200 family alone was sufficient to prevent TGF- β -induced EMT. Together, these microRNAs cooperatively regulate expression of the E-cadherin transcriptional repressors ZEB1 (also known as δ EF1) and SIP1 (also known as ZEB2), factors previously implicated in EMT and tumour metastasis. Inhibition of the microRNAs was sufficient to induce EMT in a process requiring upregulation of ZEB1 and/or SIP1. Conversely, ectopic expression of these microRNAs in mesenchymal cells initiated mesenchymal to epithelial transition (MET). Consistent with their role in regulating EMT, expression of these microRNAs was found to be lost in invasive breast cancer cell lines with mesenchymal phenotype. Expression of the miR-200 family was also lost in regions of metaplastic breast cancer specimens lacking E-cadherin. These data suggest that downregulation of the microRNAs may be an important step in tumour progression.

MicroRNAs are small, non-coding RNAs that modulate gene expression post-transcriptionally. In metazoa, they act predominantly to inhibit translation of their specific targets, but they also typically cause a modest reduction in the level of their target mRNAs^{1,2}. Hundreds of microRNAs have been identified in vertebrates, with varying patterns of expression that range from ubiquitous to highly tissue- or developmental-stage-restricted. In some cases, an individual microRNA can act as

a developmental switch by regulating a key target mRNA³. Speculating that switching between cell phenotypes that occurs during EMT may be specified to some extent by microRNAs, we searched for microRNAs whose expression changed during EMT. To this end, we used an *in vitro* model of EMT, which was generated by stable transfection of Madin Darby canine kidney (MDCK) epithelial cells with the protein tyrosine phosphatase Pez (PTP-Pez). Overexpression of PTP-Pez caused MDCK cells to undergo EMT, as indicated by loss of E-cadherin expression, gain in expression of the mesenchymal markers fibronectin, ZEB1 and SIP1, loss of cohesion, induction of cell motility and a change in cell morphology⁴ (Fig. 1a). Using microarrays to compare microRNA levels in MDCK and MDCK-Pez cells, we found that all five members of the miR-200 family and miR-205 were markedly downregulated in the MDCK-Pez cells (Fig. 1b). The miR-200 family are clustered at two locations in the genome (Fig. 1c), providing a possible explanation for their co-regulation, and are highly related in sequence (Fig. 1d). Using quantitative real-time PCR assays, we confirmed that all five members of the miR-200 family, as well as miR-205, were downregulated by more than 100-fold in the mesenchymal MDCK-Pez cells, whereas a selection of other microRNAs were confirmed to be largely unchanged (Fig. 1e).

To verify that downregulation of the miR-200 family and miR-205 is characteristic of EMT, and not an unrelated consequence of PTP-Pez overexpression, we examined their regulation in cells induced to undergo EMT in response to TGF- β . MDCK cells treated with TGF- β 1 underwent a morphological change (Fig. 2a) with loss of cohesion, a decline in the expression of E-cadherin and induction of the mesenchymal markers fibronectin, N-cadherin, ZEB1 and SIP1 (Fig. 2b). The miR-200 family and miR-205 were selectively downregulated (Fig. 2c), indicating that they are involved in TGF- β -induced EMT. To determine whether the miR-200 downregulation is essential for the TGF- β response, we generated MDCK cells that constitutively express either the miR-200b-200a-429 cluster or the miR-200c-141 cluster by transduction with lentivirus

¹Hanson Institute and Division of Human Immunology, Institute of Medical and Veterinary Science, Adelaide, SA 5000, Australia. ²Discipline of Paediatrics, School of Paediatrics and Reproductive Health, University of Adelaide, Adelaide SA 5005 and Women's and Children's Health Research Institute, Adelaide, SA 5006, Australia.

³Division of Tissue Pathology, Institute of Medical and Veterinary Science, Adelaide, SA 5000, Australia. ⁴Discipline of Medicine, The University of Adelaide, Adelaide, SA 5005, Australia. ⁵School of Molecular and Biomedical Sciences, The University of Adelaide, Adelaide, SA 5005, Australia. ⁶Current address, Centenary Institute of Cancer Medicine and Cell Biology, University of Sydney, Newtown, NSW 2042, Australia.

⁷These authors contributed equally to this study.

⁸Correspondence should be addressed to G.G. (e-mail: greg.goodall@imvs.sa.gov.au)

Received 15 January 2008; accepted 10 March 2008; published online 30 March 2007; DOI: 10.1038/ncb1722

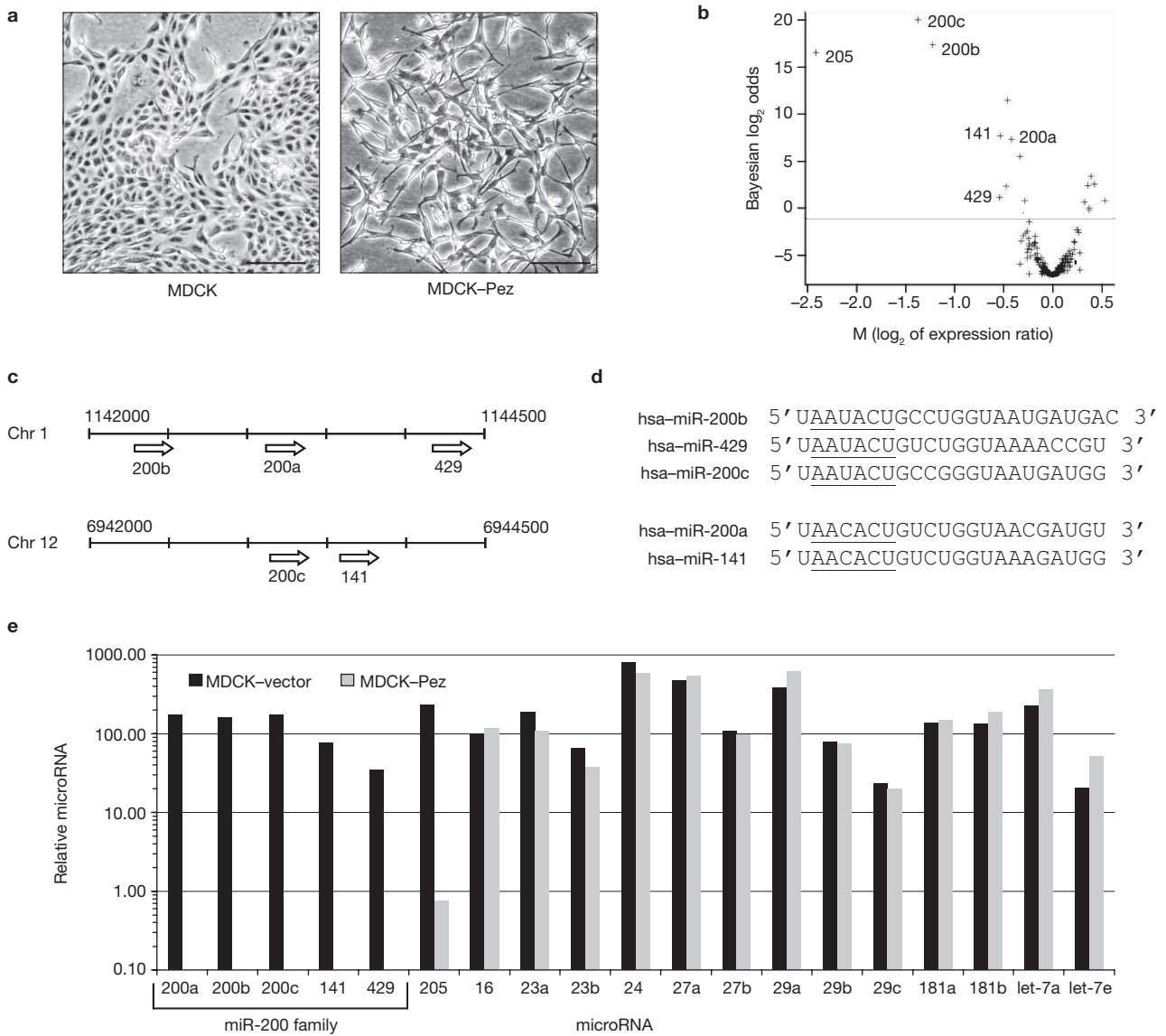


Figure 1 Identification of microRNAs that are regulated during EMT. (a) Morphology of MDCK and MDCK-Pez cells. Scale bars represent 100 μm. (b) Volcano plot showing changes in microRNAs detected by microarray of RNA from MDCK and MDCK-Pez cells. Bayesian log odds of differential expression is plotted against log₂ (expression in MDCK divided by expression in MDCK-Pez). (c) Chromosomal locations of the members

of the miR-200 family in the human genome. The same clustering is found in other vertebrates, including the dog. (d) Sequence alignment of microRNAs of the miR-200 family. Nucleotides 2–7, representing the seed sequence, are underlined. (e) Quantification of microRNAs in MDCK and MDCK-Pez cells as measured by TaqMan real-time PCR. Data are means of triplicate PCR assays.

expressing the microRNA cluster, driven by the cytomegalovirus (CMV) promoter. Enforced constitutive expression of either cluster prevented TGF-β-induced EMT (Fig. 2d, e), demonstrating that downregulation of the miR-200 family is critical for this response.

In animals, microRNA function generally involves uninterrupted base-pairing between nucleotides 2–7 (commonly called the seed sequence) of the microRNA and a complementary sequence in the 3' UTR of the target mRNA. Based on the similarity of their seed sequences, miR-200a and miR-141 are predicted to interact with the same target sites (hereafter referred to as miR-200a sites), whereas miR-200b, miR-200c and miR-429 are predicted to recognize another group of sites (hereafter referred to as miR-200b sites; Fig. 1d). The target prediction program Targetscan⁵ indicates that highly conserved binding sites for each of these

microRNAs are present in the *ZEB1* and *SIP1* mRNAs. *ZEB1* and *SIP1* are repressors of *E-cadherin* transcription that have been implicated in EMT^{6,7}. Two recent reports have implicated *ZEB1* and *SIP1* as targets of miR-200c and miR-200b respectively^{8,9}, although characterization of their interactions was incomplete. Targetscan identifies two potential miR-200b sites in the *ZEB1* mRNA, but we noticed that the Genbank Refseq entry for human *ZEB1* (NM_030751) is artificially truncated (Supplementary Information, Fig. S1). Searching the complete 3' UTR (approximately 1.9 kb) by manual inspection revealed that *ZEB1* contains three putative sites for miR-200a, five for miR-200b and one for miR-205 (Fig. 3a; Supplementary Information, Fig. S1); all are conserved between human, mouse and dog. The *SIP1* 3' UTR is predicted to contain three sites for miR-200a, six for miR-200b and two for miR-205 (Fig. 3a).

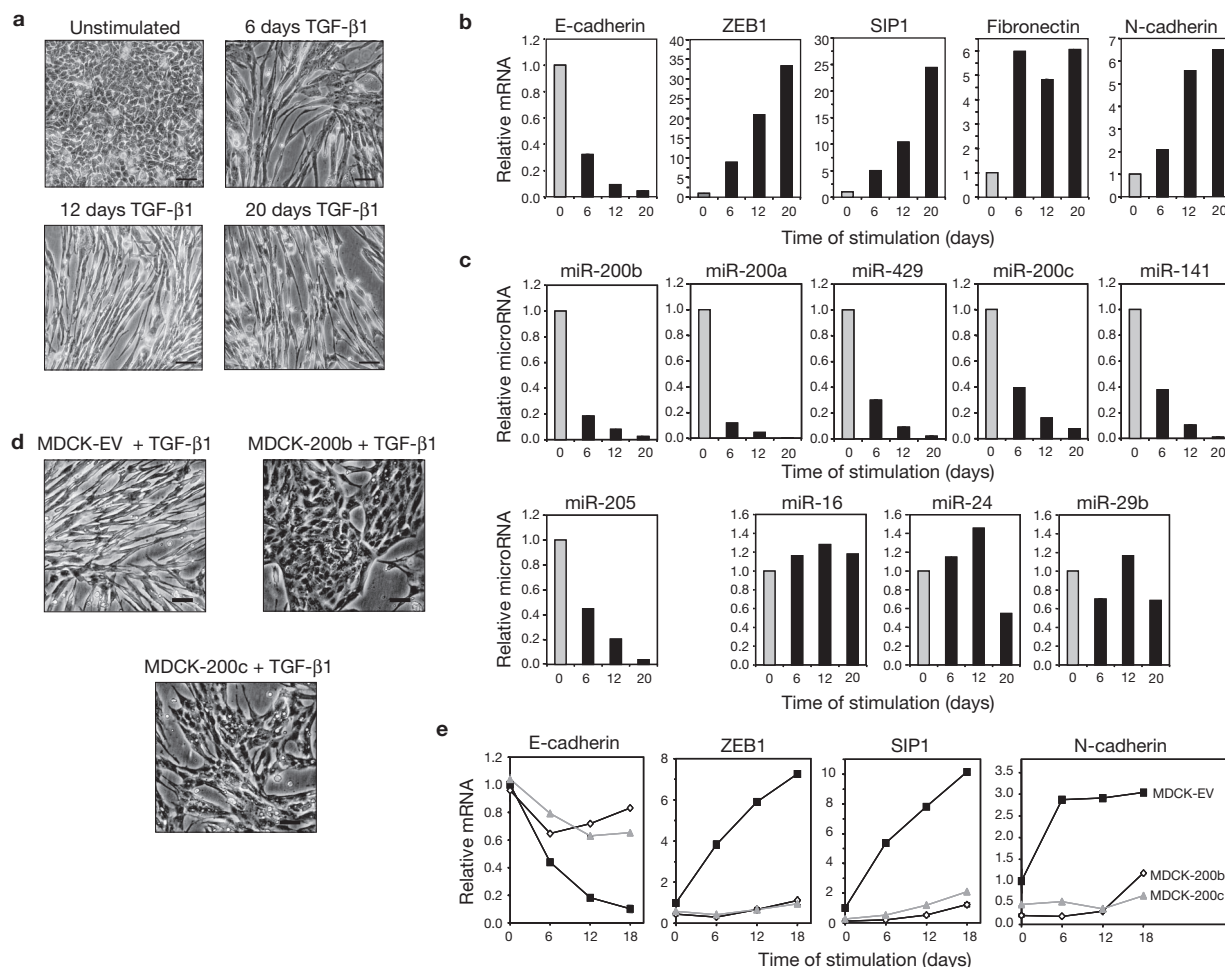


Figure 2 The miRNA-200 family and miRNA-205 are downregulated during TGF- β -mediated EMT. **(a)** Phase contrast microscopy of MDCK cells treated with TGF- β 1 over a 20-day period. Scale bars represent 50 μ m. **(b)** Changes in expression of epithelial and mesenchymal markers in MDCK cells treated with TGF- β , as measured by real-time RT-PCR. **(c)** Changes in microRNA levels in the TGF- β -treated MDCK cells, as measured by real-time locked nucleic-acid-mediated PCR (miR-200a and miR-200b) or TaqMan PCR. Three independent time courses were performed; the data are means from a single representative time course experiment measured in triplicate.

To test whether *ZEB1* and *SIP1* are targeted by microRNAs in MDCK cells, we attached their 3' UTRs to Renilla luciferase (RL) reporter genes (Fig. 3b) and compared reporter activities in MDCK and MDCK-Pez cells. Addition of the *ZEB1* and *SIP1* 3' UTRs to the luciferase reporter strongly repressed expression in MDCK cells, but was much less inhibitory in MDCK-Pez cells (Fig. 3c), whereas control reporters were equally expressed in both cell types. These results are consistent with the *ZEB1* and *SIP1* 3' UTRs being targeted by microRNAs in MDCK cells.

To verify that the miR-200 family repress the *RL-ZEB1* and *RL-SIP1* reporters, we cotransfected synthetic microRNA precursors (Pre-miRs) with the reporter genes into MDCK-Pez cells. The minimum effective concentration of Pre-miR, determined by titrating the miR-200b Pre-miR, was found to be 4 nM (Supplementary Information, Fig. S2). Cotransfection with miR-200b had a marked repressive effect on both *RL-ZEB1* and *RL-SIP1*, inhibiting expression by approximately 90% (Fig. 3d). MiR-200a and miR-205 inhibited *RL-SIP1* and *RL-ZEB1* by

25–60%, the effectiveness of each microRNA being roughly proportional to its number of putative target sites. Mutation of the miR-200b sites in *ZEB1* and *SIP1* prevented downregulation of the reporters by miR-200b (Fig. 3d), verifying that the effect of the microRNA is due to direct interaction with the binding sites in the 3' UTRs. The mutations also reduced the repression by endogenous microRNAs in MDCK cells (Fig. 3c). To assess the repressive effect of the endogenous microRNAs, we measured reporter activity in MDCK cells in the presence of antisense inhibitors of the microRNAs. Inhibition of miR-200b alone relieved some of the repression caused by the *ZEB1* and *SIP1* 3' UTRs, but maximal relief of repression was obtained by cotransfecting cells with a combination of the microRNA inhibitors (Fig. 3e). This confirmed that endogenous microRNAs of this family do indeed repress *ZEB1* and *SIP1*, and showed that miR-200a, miR-200b and miR-205 do so in a cooperative manner. On the basis of the preceding observations, we surmised that a function of miR-205 and the miR-200 family is to prevent expression of

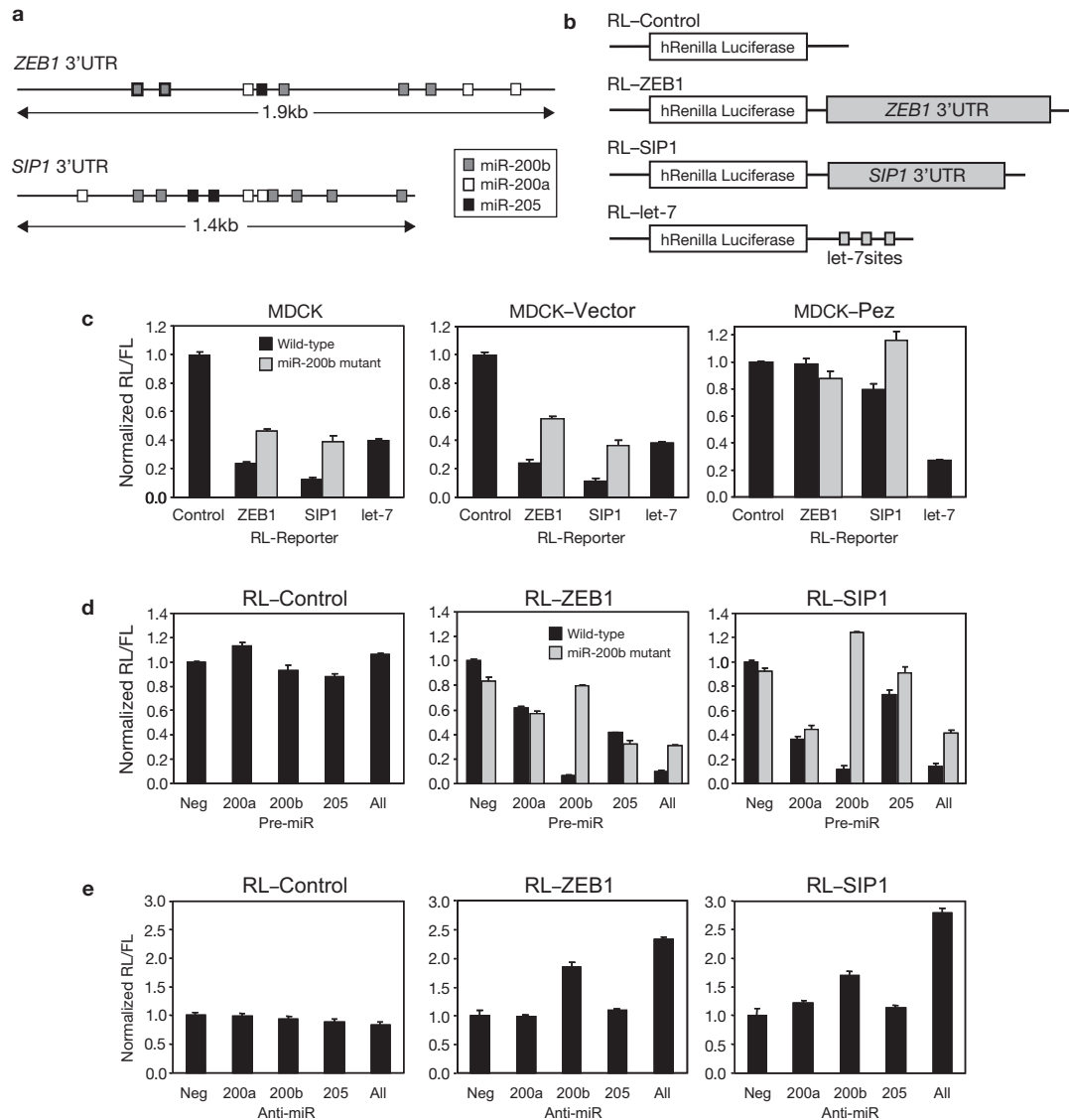


Figure 3 *ZEB1* and *SIP1* 3'UTRs are regulated by miR-200a, miR-200b and miR-205. (a) Schematic of predicted miR-200a, miR-200b and miR-205 sites in the human *ZEB1* and *SIP1* 3'UTRs. (b) Schematic representation of the reporter constructs. RL-let-7 contains 3 artificial let-7 sites³⁵. The let-7 microRNAs were expressed at similar levels in MDCK and MDCK-Pez cells (Fig. 1e). (c) The RL reporter plasmids (RL-control, RL-let-7, RL-ZEB1, RL-ZEB1 miR-200b mutant, RL-SIP1 and RL-SIP1 miR-200b mutant) were transiently transfected into MDCK, MDCK-vector or MDCK-Pez cells, along with a firefly luciferase reporter (pGL3 control) for normalization. Luciferase activities were measured after 48 h. The data are mean \pm s. e. m. of separate transfections ($n = 6$), and are shown as the ratio of RL activity to firefly

luciferase activity. (d) MDCK-Pez cells were cotransfected with the RL reporters and 4 nM of synthetic miR-200a, miR-200b and miR-205 precursors (Pre-miR, Ambion) either separately or in combination (All). Luciferase activities were measured after 48 h. Data are expressed relative to the activity in cells transfected with a negative-control Pre-miR (Neg). The data are mean \pm s. e. m. of separate transfections ($n = 6$). (e) MDCK cells were cotransfected with the RL reporters and 30 nM of miR-200a, miR-200b and miR-205 inhibitors (Anti-miR, Ambion) either separately or in combination (All). Luciferase activities were measured after 48 h. Data are expressed relative to the activity in cells transfected with a negative control Pre-miR (Neg). The data are mean \pm s. e. m. of separate transfections ($n = 6$).

ZEB1 and *SIP1* in epithelial cells, which may otherwise trigger EMT by downregulating *E-cadherin*, and further, that downregulation of the microRNAs may be sufficient to initiate EMT. To test this, we examined the effect of the microRNA inhibitors on cell phenotype. After 6 days of transfection with a miR-200b inhibitor or a combination of miR-200a, miR-200b and miR-205 inhibitors, the MDCK cells had begun to adopt a mesenchymal-like morphology, the characteristics of which intensified over a 19-day time course. Among these changes in characteristics, we observed an elongated cell morphology, loss of *E-cadherin* and *ZO-1* expression from the plasma membrane, and

rearrangement of the actin cytoskeleton from a cortical to a stress-fibre pattern (Fig. 4a). *ZEB1*, *SIP1*, *fibronectin* and *N-cadherin* mRNAs were progressively induced and *E-cadherin* mRNA was reduced, with maximal effects observed at day 19 (Fig. 4b). The level of *ZEB1* and *SIP1* mRNA induction after inhibition of all three microRNAs was 2-fold greater than with miR-200b alone, indicating that the effect of combining the microRNAs is synergistic; this was confirmed at the protein level for *ZEB1* (Fig. 4c) and mirrors the results observed with the RL-ZEB1 and RL-SIP1 reporters (Fig. 3e). We also investigated whether EMT was accompanied by a change in cell motility, using a

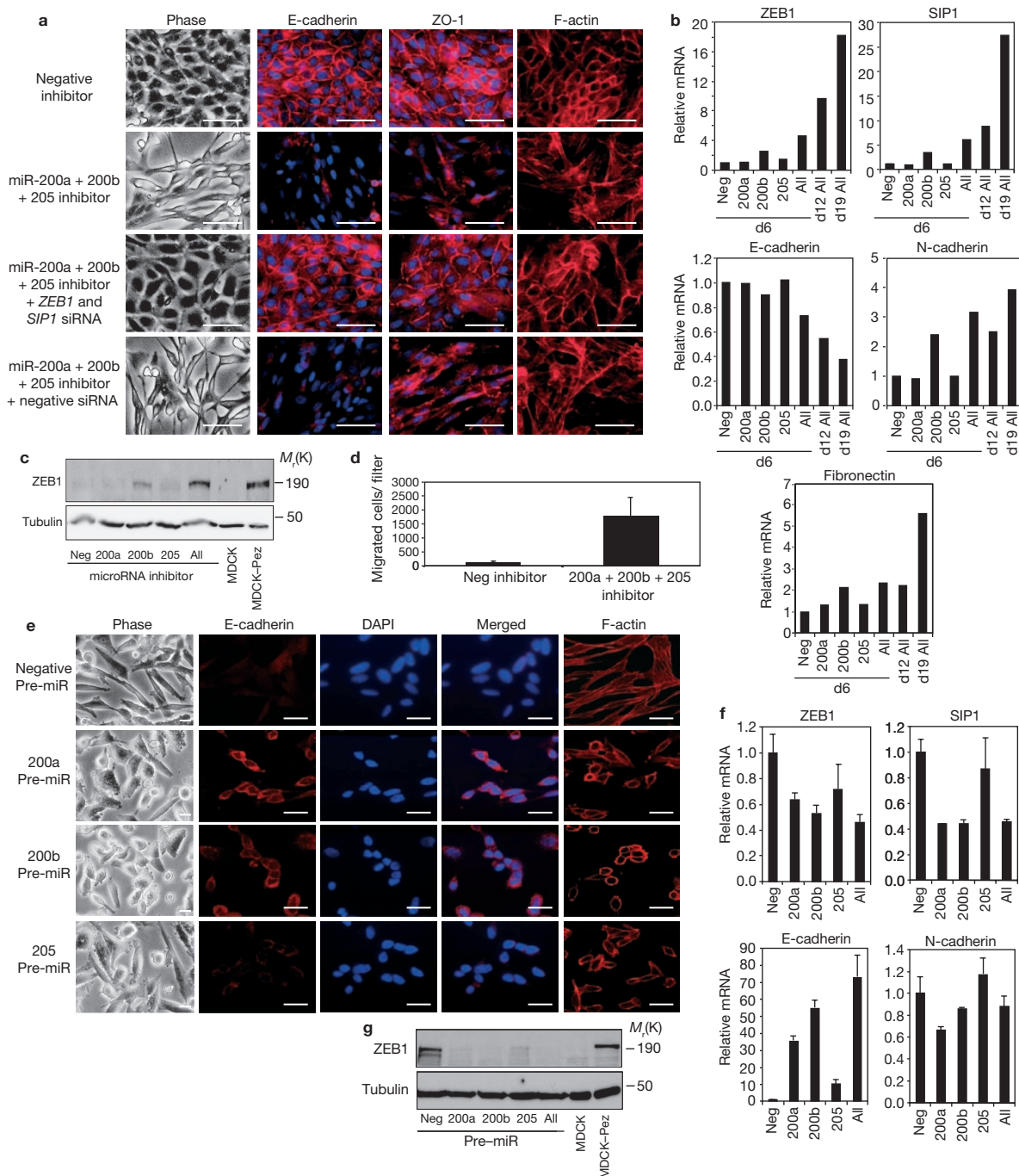


Figure 4 Manipulation of the miR-200 family and miR-205 levels can induce EMT or MET. **(a)** Phase contrast microscopy (left panel) and E-cadherin, ZO-1 and F-actin staining (right panels) of MDCK cells transfected with a negative control or combination of miR-200a, miR-200b and miR-205 inhibitors for 12 days. DAPI staining was used to detect nuclei and is merged with E-cadherin and ZO-1 in their respective panels. The scale bar represents 50 μ m. **(b)** Quantification by real-time PCR of EMT markers in MDCK cells transfected with microRNA inhibitors over a 19-day time course. Data from days 6, 12 and 19 are shown. MicroRNA inhibitors were transfected either separately or in combination (All) with the results expressed relative to a negative-control inhibitor (Neg). The data are means of two independent experiments with all measurements made in triplicate. **(c)** Immunoblot of ZEB1 and tubulin in cells transfected with microRNA inhibitors for 6 days. For comparison, the levels of ZEB1 in MDCK and MDCK-Pez cells are shown. **(d)** Migration towards serum of MDCK cells transfected with a negative-control microRNA inhibitor or a

combination of inhibitors of miR-200a, miR-200b and miR-205, 9 days post-transfection. Data are means \pm s. e. m. of 3 separate migration assays from 2 independent experiments ($n = 6$). **(e)** Phase contrast microscopy (left panel) and E-cadherin and F-actin staining (right panels) of MDCK-Pez cells transfected with synthetic miR-200a, miR-200b and miR-205 precursors (Pre-miR) for 3 days. DAPI staining was used to detect nuclei and combined with the E-cadherin stained image in the merged panel. Scale bars represent 10 μ m. **(f)** Quantification by real-time PCR of EMT markers in MDCK-Pez cells transfected with microRNA precursors for 3 days. MicroRNAs were transfected either separately or in combination (All), with the results expressed relative to a negative-control precursor (Neg). The data are mean \pm s. d. of three transfection experiments with quantitative PCR, performed in duplicate ($n = 3$). **(g)** Immunoblot of ZEB1 and tubulin in cells transfected with microRNA precursors from the experiment above. For comparison, the levels of ZEB1 in MDCK and MDCK-Pez cells are shown. Full scans of immunoblots are shown in Supplementary Information, Fig. S5.

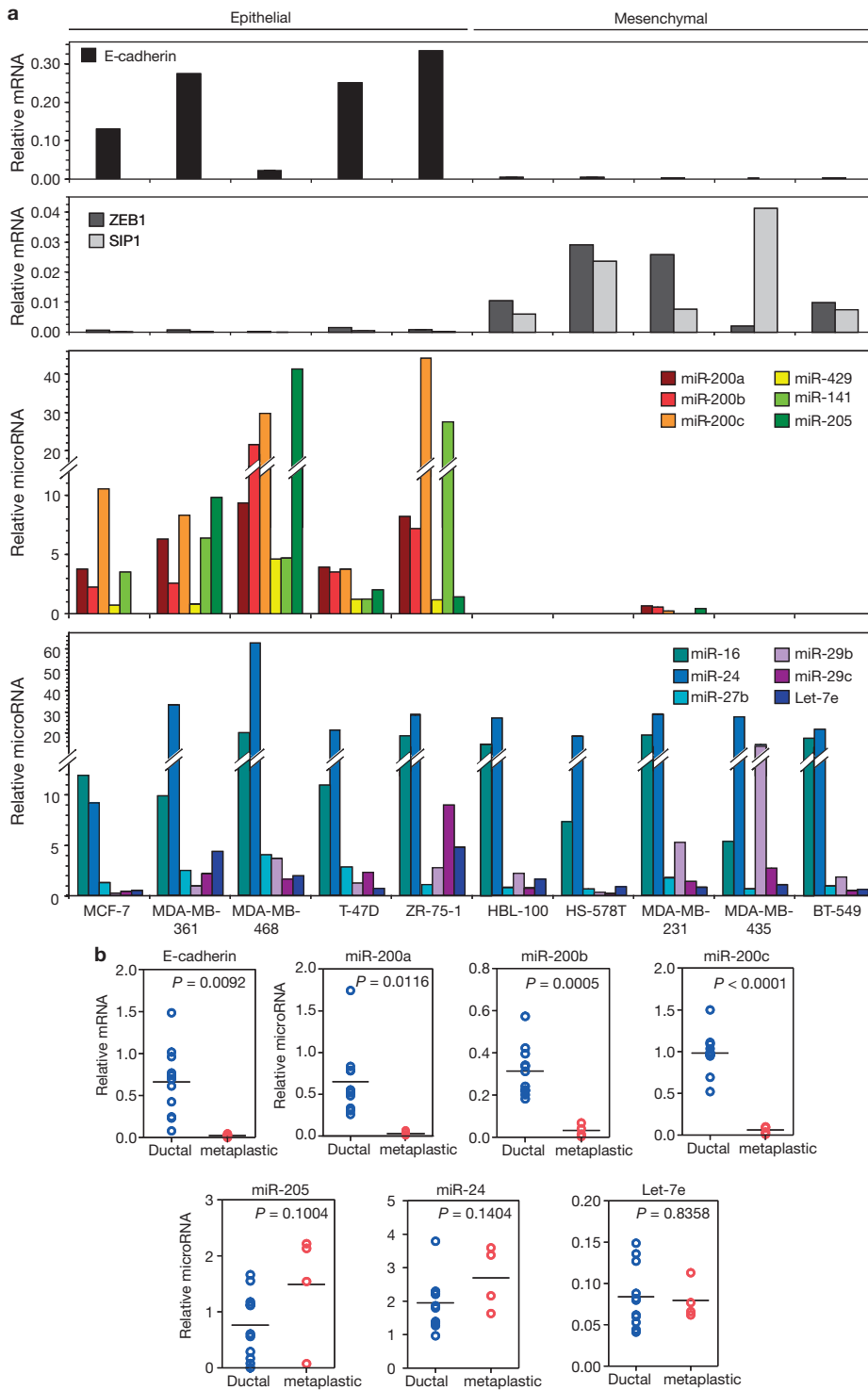


Figure 5 MicroRNA levels are associated with mesenchymal phenotype. (a) MicroRNAs and *E-cadherin*, *ZEB1*, and *SIP1* mRNAs levels were measured by real-time PCR in breast cancer cell lines with predominantly epithelial or mesenchymal features, as indicated. Data are means of triplicate measurements. (b) Measurement of *E-cadherin* and microRNAs in

ductal ($n = 11$) and sarcomatoid metaplastic ($n = 4$) primary breast cancer specimens was performed using real-time PCR. The data represent at least triplicate measurements from single RNA samples. MicroRNA levels are normalized to miR-16. P values were calculated using a two-tailed Student's t -test. The mean value for each data set is shown as a horizontal line.

Transwell migration assay. Inhibition of the microRNAs with antisense oligonucleotides caused an increase in the migration of cells (>10-fold, Fig. 4d), further demonstrating that these cells had gained functional mesenchymal characteristics.

Having found that miR-200 family expression is necessary for maintenance of the epithelial phenotype, we next asked whether ectopic expression of the microRNAs in mesenchymal cells would promote MET, the reverse of EMT. Transfection of MDCK-Pez cells

with miR-200a, miR-200b or miR-205 (Pre-miRs) caused the cells to undergo a morphological change from the spindle-shaped, mesenchymal form to a rounded, epithelial-like form, with many cells aggregating together in groups (Fig. 4e). Immunofluorescent staining of these cells for E-cadherin revealed expression was induced and E-cadherin localized to the plasma membrane, typical of the pattern observed in epithelial cells (Fig. 4e). The degree of induction correlated with the ability of that microRNA to upregulate *E-cadherin* mRNA levels (Fig. 4f). In addition, F-actin distribution was rearranged in these cells from a stress-fibre to a cortical pattern, another hallmark of the epithelial phenotype (Fig. 4e). To confirm that the epithelial-like reversion in cell morphology was due to downregulation of ZEB1 and SIP1, we measured mRNA and, in the case of ZEB1, protein levels in these samples. Ectopic expression of miR-200a or miR-200b reduced *ZEB1* mRNA (Fig. 4f), and reduced ZEB1 protein even more markedly (Fig. 4g), providing further evidence of a direct repression of ZEB1 by the microRNAs. *SIP1* mRNA levels were similarly reduced (Fig. 4f), consistent with it also being directly regulated by the microRNAs. In accordance with downregulation of ZEB1 and SIP1, we observed a proportional increase in the level of *E-cadherin* mRNA, indicative of their influence on *E-cadherin* transcription. This increase in *E-cadherin* was also accompanied by a modest decrease in the mesenchymal marker *N-cadherin* (Fig. 4f). Taken together, these data indicate that the miR-200 family can induce a MET-like reversion of MDCK–Pez cells.

To determine whether ZEB1 and SIP1 are the key mediators of EMT induced by microRNA repression, we performed microRNA inhibition experiments in the presence of two different combinations of *ZEB1* and *SIP1* short interfering (si) RNAs designed to prevent upregulation of these proteins. The effectiveness and specificity of each siRNA in reducing *ZEB1* and *SIP1* mRNA levels were initially confirmed by transfection into MDCK–Pez cells (Supplementary Information, Fig. S3). Knockdown of both *ZEB1* and *SIP1* in these cells, but not single knockdown of one or the other, was required to induce E-cadherin expression and an MET-like morphological change, indicating a redundancy in their function (Supplementary Information, Fig. S3). Simultaneous knockdown of *ZEB1* and *SIP1* prevented the induction of EMT by antisense inhibitors of miR-200a, miR-200b and miR-205 in MDCK cells, as demonstrated by maintenance of E-cadherin, ZO-1 and cortical F-actin expression at the plasma membrane (Fig. 4a). Additionally, these siRNAs prevented downregulation of *E-cadherin* mRNA and upregulation of *fibronectin* and *N-cadherin* mRNAs (Supplementary Information, Fig. S3). These data confirm that ZEB1 and SIP1 are the primary factors through which these microRNAs mediate their effect on cell phenotype. The pronounced change in *ZEB1* and *SIP1* mRNA levels that occurred on prolonged exposure to TGF- β treatment (Fig. 2b) suggests that feedback mechanisms and/or additional regulation upstream of ZEB1 and SIP1 may also contribute to setting the complete genetic programme.

Several studies using *in vivo* mouse-model systems have suggested that EMT is involved in breast cancer metastasis^{10–12}. In addition, the invasiveness of commonly used breast cancer cell lines is often correlated with their mesenchymal state¹³. To investigate whether the regulation of EMT and invasive capacity by the miR-200 family may extend to breast cancer cells, we analysed the expression of E-cadherin, ZEB1, SIP1 and microRNAs in ten commonly used human breast cancer cell lines. The cell lines that express E-cadherin and retain the features of

well-differentiated epithelial cells were found to express the miR-200 family and miR-205, whereas cells that are invasive and generally mesenchymal in phenotype expressed low to undetectable levels of the miR-200 family and miR-205 (Fig. 5a). As expected from their level of miR-200 family expression, the epithelial cells expressed barely detectable levels of both ZEB1 and SIP1, whereas the opposite was observed in the more mesenchymal cells. Remarkably, this reciprocal pattern is also conserved across the entire NCI60 set of cancer cell lines¹⁴. We also measured microRNA levels in several human primary breast cancers. These included typical invasive ductal carcinomas, which exhibit an epithelial phenotype, and metaplastic breast cancers, which are a well recognized, albeit rare, subtype of breast cancer that contains both mesenchymal (sarcomatoid) and epithelial (epithelioid) regions (Supplementary Information, Fig. S4). In addition to possessing mesenchymal characteristics, recent microarray profiling of metaplastic cancers has shown that their expression profile is distinct from ductal carcinomas and is associated with EMT-like changes¹⁵. We found that ductal tumours expressed significantly higher levels of E-cadherin, compared with sarcomatoid metaplastic tumours (Fig. 5b; Supplementary Information, Fig. S4). The ductal tumours expressed approximately 10–22-fold higher levels of the miR-200 family than sarcomatoid metaplastic tumours (Fig. 5b), with a significant correlation between microRNA and E-cadherin levels across both tumour types (Supplementary Information, Fig. S4). In contrast, there was no significant difference in the expression of miR-16 (used for normalizing), miR-24 and let-7e between the two tumour types (Fig. 5b) and their levels did not correlate with that of E-cadherin (Supplementary Information, Fig. S4). MiR-205 levels were highly variable across both tumour types and did not relate to E-cadherin expression (Fig. 5b). A recent report found that miR-205 is expressed in the myoepithelial basal cell compartment of the breast, but downregulated in matching tumours, suggesting that this microRNA may be lost in the early stages of tumour progression¹⁶. Although the origin of metaplastic carcinoma is not well understood, the presence of epithelial and mesenchymal components in the same tumour suggests an EMT-like involvement¹⁷ (Supplementary Information, Fig. S4). This is supported by our finding that the miR-200 family is absent in the mesenchymal sarcomatoid regions. This, together with the consistent loss of the miR-200 family in mesenchymal-like breast cancer cell lines, indicates that loss of the miR-200 family may contribute to the progression of some breast cancers.

Our findings of an important role for the miR-200 family and miR-205 in enforcing the epithelial phenotype are supported by microRNA expression surveys across numerous tissue types and organisms. MiR-200a and miR-200b expression is enriched in tissues where epithelial cell types predominate in humans^{18–20} and zebrafish²¹. In the chick embryo, miR-200a, miR-200b and miR-205 expression is confined to the endoderm and ectoderm²², but largely excluded from the mesoderm, an area where ZEB1 and SIP1 are prominently expressed during development^{23,24}. Furthermore during skin morphogenesis, all members of the miR-200 family and miR-205 are highly expressed in the epidermis²⁵. Collectively, these observations suggest an involvement of the miR-200 family and miR-205 in establishing epithelial cell lineages during early development.

In addition to being essential for embryonic development, EMT has also been implicated in tumour metastasis; a key step in this process involves the downregulation of E-cadherin^{17,26}. ZEB1 and SIP1 are able to initiate EMT by binding to E-boxes within the *E-cadherin* promoter and

repressing its transcription²⁷. The relative contribution of each repressor in tumorigenesis seems to depend on the cellular context. ZEB1 is implicated in the progression of lung, colon and uterine cancers^{28–30}. In colon cancer, upregulation of ZEB1 selectively occurred within dedifferentiated cells at the invasive front of the tumour and was associated with loss of the basement membrane, EMT and poor patient-survival³⁰. This suggests that ZEB1 has a direct role in metastasis. SIP1 has been linked with low E-cadherin expression in breast cancer cell lines³¹, an observation also supported by our data. Together these findings indicate that ZEB1 and SIP1 are critical promoters of cancer progression. Our finding that ZEB1 and SIP1 expression is controlled by the miR-200 family and miR-205 suggests that downregulation of these microRNAs is an essential early step in tumour metastasis. □

METHODS

Cell culture. All cell lines, with the exception of MDA-MB-435 and BT-549, were maintained in Dulbecco's modified Eagle's medium (DMEM; Invitrogen) supplemented with 10% fetal bovine serum (FBS). MDA-MB-435 cells were maintained in alpha modified Eagle's medium (αMEM; Invitrogen) supplemented with 5% FBS. BT-549 cells were maintained in RPMI 1640 (Invitrogen) supplemented with 10% FBS. The MDCK–Pez and MDCK–vector stable cell lines were generated by stable transfection of PTP–Pez or empty vector, respectively, into MDCK cells⁴. A single MDCK–Pez clone was used for all of the experiments, with the exception of the microarray experiments (detailed below). TGF-β-stimulation experiments were performed with recombinant human TGF-β1 (5 ng ml⁻¹; R&D systems). Unstimulated MDCK cells were split once a week at a 1:10 ratio, whereas TGF-β-treated cells were split twice a week at a ratio of 1:5 to retain cell viability.

RNA extraction and real-time PCR. Total RNA was extracted using Trizol (Invitrogen), according to the manufacturer's instructions. For mRNA analysis, complementary DNA (cDNA) was randomly primed from 2.0 μg of total RNA using the Omniscript reverse transcription kit (Qiagen). Real-time PCR was subsequently performed in triplicate with a 1:4 dilution of cDNA using the Quantitect SyBr green PCR system (Qiagen) on a Rotorgene 6000 series PCR machine (Corbett Research). Data were collected and analysed using the Rotorgene software accompanying the PCR machine. Relative expression levels were determined using the comparative quantification feature of the Rotorgene software. All mRNA quantification data were normalized to GAPDH. For microRNA analysis, real-time PCR was performed as above, using TaqMan microRNA assays according to the manufacturer's instructions (Applied Biosystems), or where specified, using locked nucleic-acid-mediated real-time PCR³². All microRNA data are expressed relative to a U6 small nuclear (sn) RNA TaqMan PCR performed on the same sample, unless otherwise specified.

MicroRNA microarray. MicroRNA microarrays were synthesized by spotting of cDNA probes to 377 microRNAs (mirVana miRNA probe set v1; Ambion) in quadruplicate onto Corning epoxide-coated slides. Samples from Trizol-extracted RNA (20 μg) were enriched for microRNA using the flashPAGE fractionator system (Ambion) and subsequently labelled for hybridization using the mirVana miRNA labelling kit (Ambion). Three competitive hybridization experiments were performed in duplicate using enriched microRNA fractions pooled from four independent MDCK–vector clones and eight independent MDCK–Pez clones. Arrays were scanned using a GenePix 4000B Scanner driven by GenePix Pro 4.0 (Molecular Devices). All analyses were performed in the freely available statistical programming and graphics environment R (<http://cran.r-project.org>). Differentially expressed miRNAs were identified using the empirical Bayes approach which ranks genes on a combination of magnitude and consistency of differential expression³³.

Generation of MDCK miR-200 family stable cell lines. Fragments containing the miR-200b–200a–429 and miR-200c–141 genomic clusters were amplified by PCR and directionally cloned into the *EcoRI* and *AvrII* sites of pLenti4.1EX. Lentivirus was generated by cotransfection of the above constructs with packaging plasmids into HEK293T cells, as described previously³⁴. MDCK cells were transduced and subsequently FACS-sorted for green fluorescent protein (GFP), which is co-expressed on a single transcript with the microRNAs.

ZEB1 and SIP1 3'UTR reporter analysis. The 3'UTRs of *ZEB1* and *SIP1* were amplified by PCR from HEK293 genomic DNA and cloned into the *XbaI* site downstream of RL in a CMV-driven RL reporter (pCI-neo-hRL³⁵). Mutations in the miR-200b seed regions of the *ZEB1* and *SIP1* 3'UTRs were generated using the QuikChange Multi site-directed mutagenesis kit (Stratagene). RL reporter plasmids (3.6 fmol) and pGL3-control (500 ng for normalization; Promega) were transfected with Lipofectamine 2000 (Invitrogen) into MDCK, MDCK–vector and MDCK–Pez cells seeded in 24-well plates (6 × 10⁴ cells per well). The total amount of DNA in each transfection was made up to 1.0 μg with the unrelated pBS-SK Bluescript (+) plasmid (Stratagene). Cells were collected after 48 h for assay using the Dual-Luciferase reporter assay system (Promega). For cotransfection experiments, 4 nM of synthetic microRNAs (Pre-miR, Ambion) or 30 nM microRNA inhibitor (Anti-miR, Ambion) were added to the above reactions. All experiments were performed in triplicate with data pooled from at least two independent experiments.

Transfection of microRNA precursors and inhibitors. MDCK–Pez cells were seeded at 6 × 10⁴ cells per well in 24-well plates and transfected with synthetic microRNAs at a final concentration of 60 nM (20 nM of each of miR-200a, miR-200b and miR-205 Pre-miRs, Ambion) using HiPerFect transfection reagent (Qiagen). Total RNA and protein were collected for assay 3 days post-transfection. MDCK cells were seeded at 1.5 × 10⁴ cells per well in 24-well plates and transfected with microRNA inhibitors at a final concentration of 300 nM (100 nM of each of miR-200a, miR-200b and miR-205 Anti-miRs, Ambion or 2'-O-methyl modified oligonucleotides, Dharmacon) or a negative control inhibitor (300 nM) as above. After 3 days of transfection, cells were split and re-transfected with additional microRNA inhibitors; this process repeated every 3–4 days for up to a total of 19 days. Total RNA was collected from cells at 6, 12 and 19 days post-transfection; protein was also collected at Day 6. For experiments where *ZEB1* and *SIP1* were concurrently knocked down, 10 nM of each siRNA (Invitrogen; 20 nM total) or a control siRNA (siCONTROL non-targeting siRNA No. 1, Dharmacon; 20 nM) was added to the above transfections.

Immunoblotting. Extracts were prepared from transfected cells with Triton X-100 lysis buffer (50 mM HEPES, pH 7.5, 150 mM sodium chloride, 10 mM sodium pyrophosphate, 5 mM EDTA, 50 mM sodium fluoride, 1% Triton X-100 and protease inhibitor cocktail) and 50 μg fractionated on a 7.5% SDS polyacrylamide gel. After transfer onto a nitrocellulose membrane, probing was carried out with anti-ZEB1 (ZEB E-20, 1:200; Santa Cruz Biotechnology) or anti-tubulin (1:10,000; Abcam) antibodies. Membranes were exposed using the ECL method (GE Healthcare) according to the manufacturer's instructions.

Fluorescence microscopy and staining for E-cadherin, ZO-1 and F-actin. MDCK and MDCK–Pez cells were transfected with microRNA inhibitors or precursors, as described above, plated onto fibronectin-coated chamber slides (BD Biosciences) and stained at day 12 or day 3, respectively. For E-cadherin and ZO-1 staining, cells were fixed in 4% paraformaldehyde, permeabilized in 0.1% Triton X-100 and probed with a mouse-anti-E-cadherin antibody (1:500; Transduction Laboratories) or rabbit-anti-ZO-1 (1:500; Zymed) antibody. The primary antibody was detected using goat-anti-mouse-Alexa 594 or goat-anti-rabbit-Alexa 594 conjugated antibodies (1:500; Invitrogen). To detect nuclei, cells were co-stained with 4'-6-Diamidino-2-phenylindole (DAPI; Invitrogen). For F-actin staining, fixed and permeabilized cells were incubated with rhodamine phalloidin (Invitrogen) for 10 min. Cells were observed on an Olympus IX81 microscope and pictures were taken using a Hamamatsu Orca camera. Images were analysed with Olympus Cell software.

Migration assays. Migration assays were performed in triplicate using Transwell migration chambers (8 μm pore size; Costar) coated with 3.5 μg fibronectin on the top and underside of the membrane. MDCK cells transfected with microRNA inhibitors were plated 9 days post-transfection in serum-free medium (5 × 10⁴ cells per Transwell) and allowed to migrate towards a 10% FBS gradient for 4 h. Cells that remained on the top of the filter were scrubbed off and cells that had migrated to the underside of the filter were fixed in methanol and stained with DAPI. Whole filters were manually counted under fluorescence.

Analysis of primary human breast cancer samples. Access to patient tumour samples was approved by the appropriate institutional human ethics review boards. De-identified tumour samples were chosen for the study by a breast

pathologist, using archival material from the Department of Tissue Pathology at the Institute of Medical and Veterinary Science. Formalin-fixed, paraffin-embedded sections were subjected to routine haematoxylin and eosin (H & E) staining. The study pathologist circled areas of tumour on the H & E sections, aiming for pure tumour areas and excluding benign intervening tissue as far as possible. Using duplicate unstained sections, marked areas of the tumour were scraped into tubes where total RNA was isolated using the miRNeasy FFPE kit (Qiagen). Real-time PCR analysis for mRNA and microRNA were performed as described above. Immunohistochemistry for E-cadherin and cytokeratin was performed with the Benchmark XT automated system (Ventana) using mouse-anti-pan-cytokeratin (AE1-AE3; Dako) and mouse-anti-E-cadherin (ECH-6; Ventana) antibodies at 1:500 dilutions, and exposed according to the directions of the Ultraview universal DAB detection kit (Ventana). Representative photographs were taken at $\times 40$ and $\times 200$ magnification.

Oligonucleotide sequences. Sequences of PCR primers and RNA oligonucleotides used for real-time PCR, *ZEB1* and *SIP1* 3'UTR cloning, *ZEB1* and *SIP1* miR-200b seed mutagenesis, miR-200b-200a-429 and miR-200c-141 cluster cloning, microRNA knockdown, and *ZEB1* and *SIP1* knockdown are shown in Supplementary Information, Table S1.

Note: Supplementary Information is available on the Nature Cell Biology website.

ACKNOWLEDGEMENTS

The authors thank Don Newgreen for critical reading of the manuscript, Witold Filipowicz for the pCI-neo-hRL and RL-let-7 plasmids, Scott Hammond for the pLenti4.IEX plasmid, Mark van der Hoek and the Adelaide Microarray Facility for printing of the microarrays, and members of the Goodall and Khew-Goodall laboratories for helpful discussions. This work was supported by grants from the National Health and Medical Research Council of Australia (to Y. K.-G., M. A. V. and G. J. G.) and The Cancer Council South Australia (to G. J. G.). P. A. G. is supported by a Peter Doherty Training Fellowship from the National Health and Medical Research Council of Australia.

Published online at <http://www.nature.com/naturecellbiology/>

Reprints and permissions information is available online at <http://npg.nature.com/reprintsandpermissions/>

- Bagga, S. *et al.* Regulation by *let-7* and *lin-4* miRNAs results in target mRNA degradation. *Cell* **122**, 553–563 (2005).
- Lim, L. P. *et al.* Microarray analysis shows that some micro RNAs downregulate large numbers of target mRNAs. *Nature* **433**, 769–773 (2005).
- Fazi, F. *et al.* A microcircuitry comprised of microRNA-223 and transcription factors NFI-A and C/EBP α regulates human granulopoiesis. *Cell* **123**, 819–831 (2005).
- Wyatt, L., Wadham, C., Crocker, L. A., Lardelli, M. & Khew-Goodall, Y. The protein tyrosine phosphatase *Pez* regulates TGF- β , epithelial mesenchymal transition, and organ development. *J. Cell Biol.* **178**, 1223–1235 (2007).
- Lewis, B. P., Burge, C. B. & Bartel, D. P. Conserved seed pairing, often flanked by adenosines, indicates that thousands of human genes are microRNA targets. *Cell* **120**, 15–20 (2005).
- Comijn, J. *et al.* The two-handed E box binding zinc finger protein *SIP1* downregulates E-cadherin and induces invasion. *Mol. Cell* **7**, 1267–1278 (2001).
- Eger, A. *et al.* δ EF1 is a transcriptional repressor of E-cadherin and regulates epithelial plasticity in breast cancer cells. *Oncogene* **24**, 2375–2385 (2005).
- Hurteau, G. J., Carlson, J. A., Spivack, S. D. & Brock, G. J. Overexpression of the microRNA *hsa-miR-200c* leads to reduced expression of transcription factor 8 and increased expression of E-cadherin. *Cancer Res.* **67**, 7972–7976 (2007).
- Christoffersen, N. R., Silahatoglu, A., Orom, U. A., Kauppinen, S. & Lund, A. H. miR-200b mediates post-transcriptional repression of ZFH1B. *RNA* **13**, 1172–1178 (2007).
- Yang, J. *et al.* Twist, a master regulator of morphogenesis, plays an essential role in tumor metastasis. *Cell* **117**, 927–939 (2004).
- Huber, M. A. *et al.* NF- κ B is essential for epithelial-mesenchymal transition and metastasis in a model of breast cancer progression. *J. Clin. Invest.* **114**, 569–581 (2004).
- Moody, S. E. *et al.* The transcriptional repressor Snail promotes mammary tumor recurrence. *Cancer Cell* **8**, 197–209 (2005).
- Lacroix, M. & Leclercq, G. Relevance of breast cancer cell lines as models for breast tumours: an update. *Breast Cancer Res. Treat.* **83**, 249–289 (2004).
- Park, S. M., Gaur, A. B., Lengyel, E. & Peter, M. E. The miR-200 family determines the epithelial phenotype of cancer cells by targeting the E-cadherin repressors, ZEB1 and ZEB2. *Genes Dev.* advance online publication, doi:10.1101/gad.1640608 (2008).
- Lien, H. C. *et al.* Molecular signatures of metaplastic carcinoma of the breast by large-scale transcriptional profiling: identification of genes potentially related to epithelial-mesenchymal transition. *Oncogene* **26**, 7859–7871 (2007).
- Sempere, L. F. *et al.* Altered microRNA expression confined to specific epithelial cell subpopulations in breast cancer. *Cancer Res.* **67**, 11612–11620 (2007).
- Thiery, J. P. Epithelial-mesenchymal transitions in tumour progression. *Nature Rev. Cancer* **2**, 442–454 (2002).
- Thomson, J. M., Parker, J., Perou, C. M. & Hammond, S. M. A custom microarray platform for analysis of microRNA gene expression. *Nature Methods* **1**, 47–53 (2004).
- Baskerville, S. & Bartel, D. P. Microarray profiling of microRNAs reveals frequent co-expression with neighboring miRNAs and host genes. *RNA* **11**, 241–247 (2005).
- Lu, J. *et al.* MicroRNA expression profiles classify human cancers. *Nature* **435**, 834–838 (2005).
- Wienholds, E. *et al.* MicroRNA expression in zebrafish embryonic development. *Science* **309**, 310–311 (2005).
- Darnell, D. K. *et al.* Micro RNA expression during chick embryo development. *Dev. Dyn.* **235**, 3156–3165 (2006).
- Funahashi, J., Sekido, R., Murai, K., Kamachi, Y. & Kondoh, H. δ -crystallin enhancer binding protein delta EF1 is a zinc finger-homeodomain protein implicated in postgastrulation embryogenesis. *Development* **119**, 433–446 (1993).
- Miyoshi, T. *et al.* Complementary expression pattern of *Zfh1* genes *Sip1* and δ EF1 in the mouse embryo and their genetic interaction revealed by compound mutants. *Dev. Dyn.* **235**, 1941–1952 (2006).
- Yi, R. *et al.* Morphogenesis in skin is governed by discrete sets of differentially expressed microRNAs. *Nature Genet.* **38**, 356–362 (2006).
- Thiery, J. P. & Sleeman, J. P. Complex networks orchestrate epithelial-mesenchymal transitions. *Nature Rev. Mol. Cell Biol.* **7**, 131–142 (2006).
- Peinado, H., Portillo, F. & Cano, A. Transcriptional regulation of cadherins during development and carcinogenesis. *Int. J. Dev. Biol.* **48**, 365–375 (2004).
- Ohira, T. *et al.* WNT7a induces E-cadherin in lung cancer cells. *Proc. Natl Acad. Sci. USA* **100**, 10429–10434 (2003).
- Spoelstra, N. S. *et al.* The transcription factor ZEB1 is aberrantly expressed in aggressive uterine cancers. *Cancer Res.* **66**, 3893–3902 (2006).
- Spaderna, S. *et al.* A transient, EMT-linked loss of basement membranes indicates metastasis and poor survival in colorectal cancer. *Gastroenterology* **131**, 830–840 (2006).
- Lombaerts, M. *et al.* E-cadherin transcriptional downregulation by promoter methylation but not mutation is related to epithelial-to-mesenchymal transition in breast cancer cell lines. *Br. J. Cancer* **94**, 661–671 (2006).
- Raymond, C. K., Roberts, B. S., Garrett-Engele, P., Lim, L. P. & Johnson, J. M. Simple, quantitative primer-extension PCR assay for direct monitoring of microRNAs and short-interfering RNAs. *RNA* **11**, 1737–1744 (2005).
- Smyth, G. K. Linear models and empirical bayes methods for assessing differential expression in microarray experiments. *Stat. Appl. Genet. Mol. Biol.* **3**, Article3 (2004).
- Barry, S. C. *et al.* Lentivirus vectors encoding both central polypurine tract and posttranscriptional regulatory element provide enhanced transduction and transgene expression. *Hum. Gene Ther.* **12**, 1103–1108 (2001).
- Pillai, R. S. *et al.* Inhibition of translational initiation by Let-7 MicroRNA in human cells. *Science* **309**, 1573–1576 (2005).

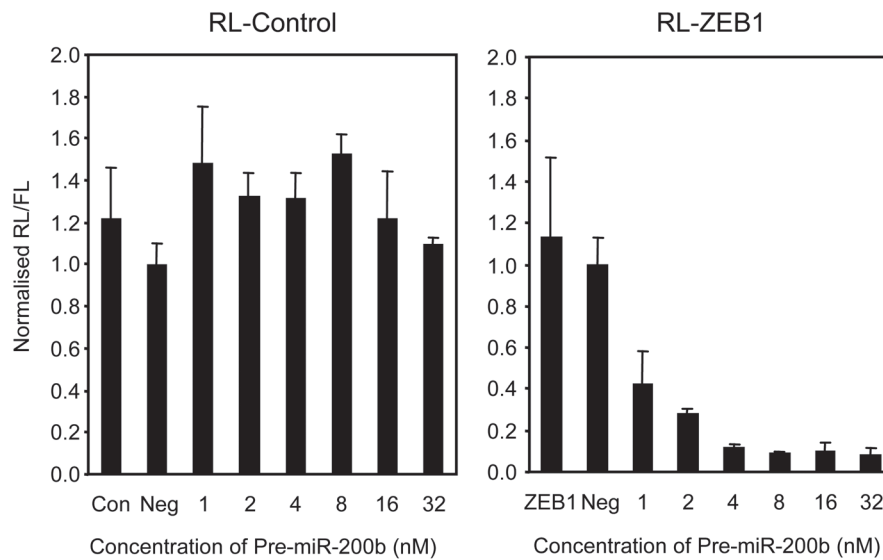


Figure S2 Determination of the minimum effective concentration of Pre-miR for inhibiting reporter expression. A range of concentrations of miR-200b Pre-miR was cotransfected with RL-Control or RL-ZEB1. Comparisons are made with samples without cotransfected microRNA (Con

or ZEB1) or cotransfected with a negative control Pre-miR (Neg). The pGL3 plasmid was cotransfected to normalise for transfection efficiency and the ratio of Renilla to Firefly luciferase activity is shown from a triplicate transfection \pm s.e.m. (n=3).

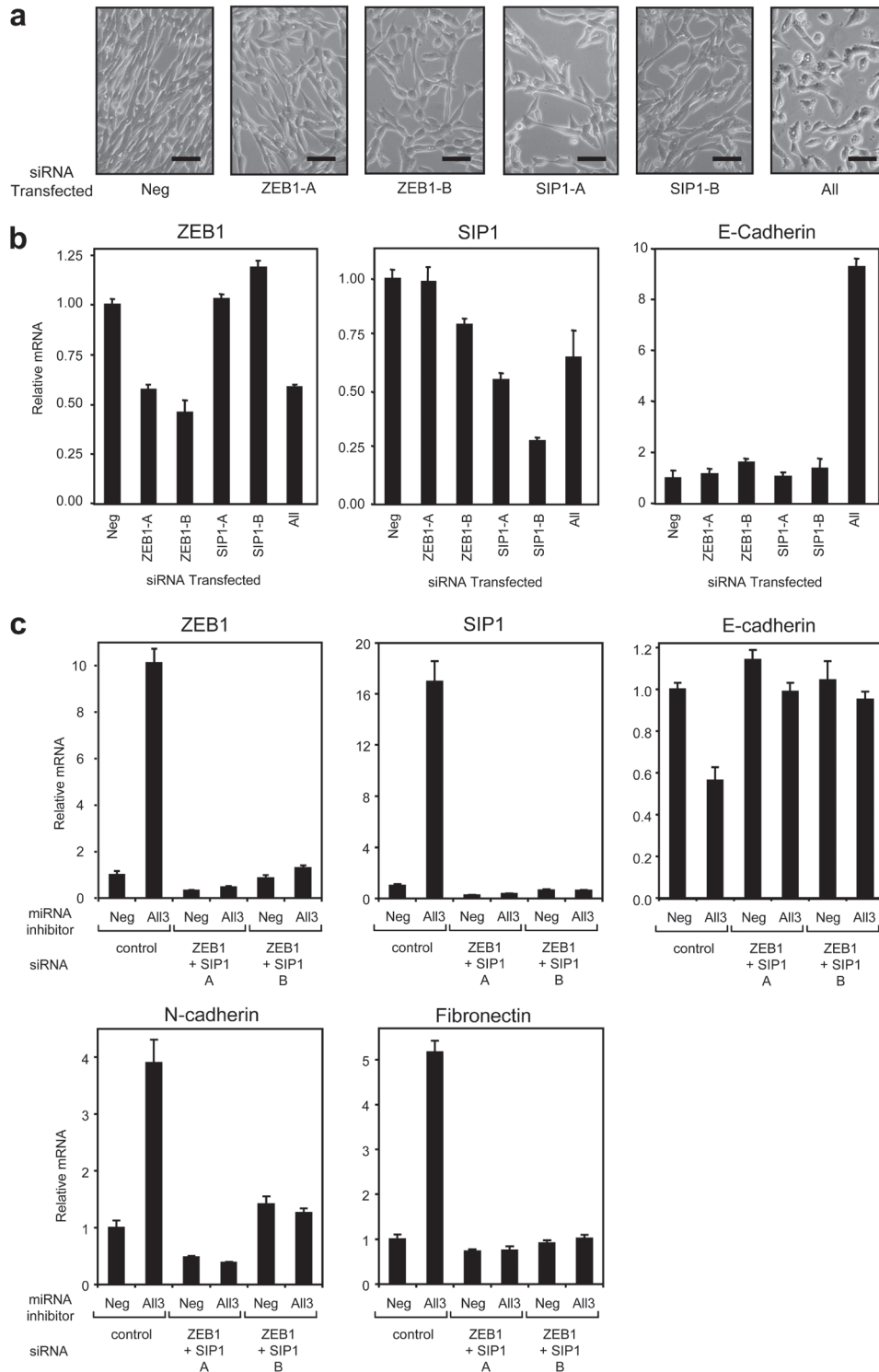


Figure S3 ZEB1 and SIP1 siRNA knockdown and their effect on MDCK-Pez cells, and EMT in MDCK cells mediated by microRNA inhibition. **(a)** Phase contrast microscopy of MDCK-Pez cells transfected with individual ZEB1 and SIP1 siRNAs (A and B) either separately or in combination (All) for 3 days. Comparisons were made with a non-targeting siRNA (Neg). Scale bars represent 50 μ m. **(b)** Quantitation by real time PCR of ZEB1, SIP1 and E-cadherin after ZEB1 and/or SIP1 knockdown. Transfections were carried out with 20 nM of each individual siRNA or 5 nM each of the four siRNAs (All).

The data are taken from a representative experiment of three transfection experiments with PCR performed in triplicate and are shown \pm s.e.m. (n=3). **(c)** Quantitation by real time PCR of EMT markers after concurrent miR-200a, miR-200b, and miR-205 inhibition (All3) or treatment with a negative control inhibitor (Neg), with or without ZEB1 and SIP1 knockdown. Successive transient transfections were performed at 3-4 day intervals for a total of nineteen days. The data are taken from two transfection experiments with qPCR performed in triplicate and are shown \pm s.e.m. (n=6).

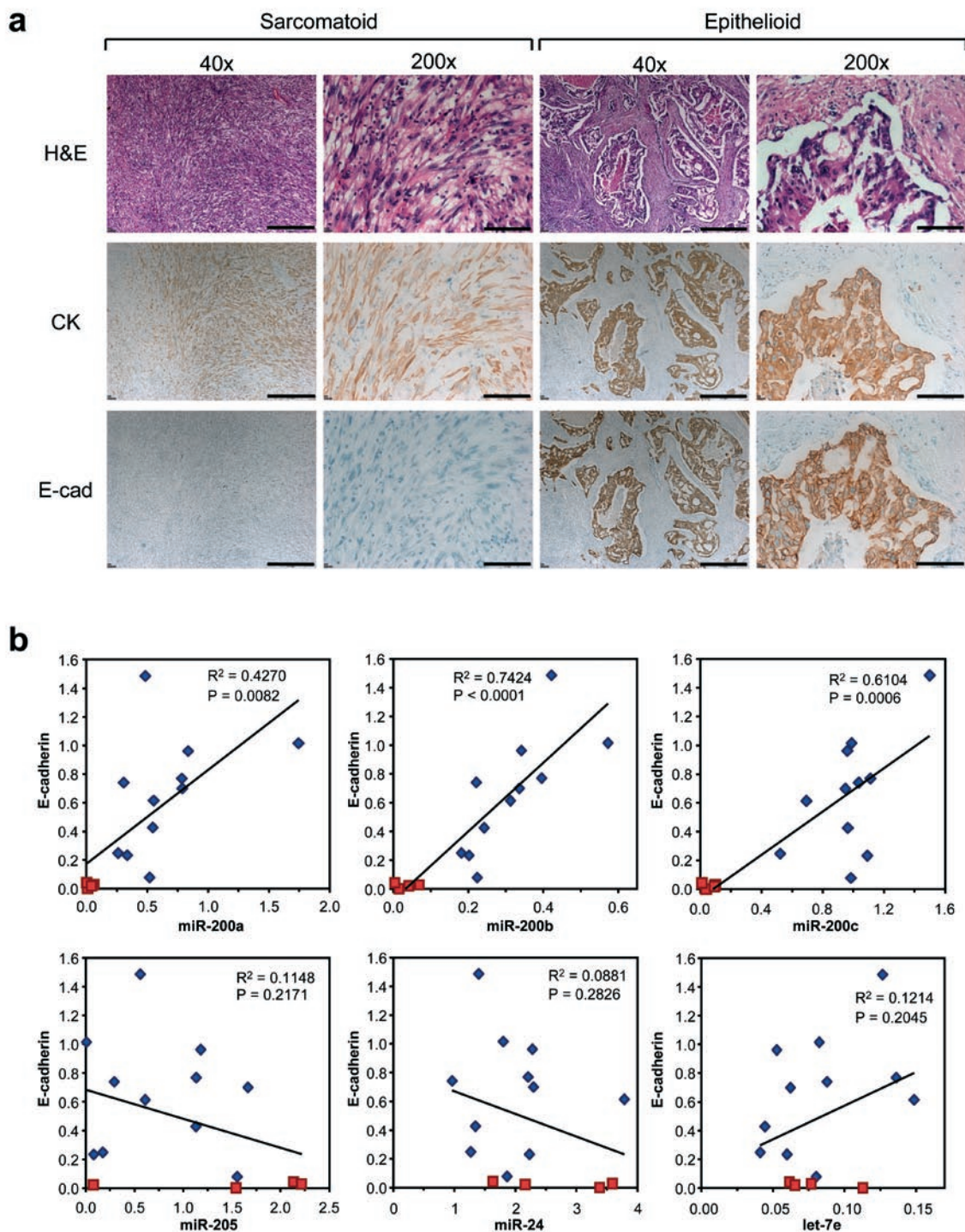


Figure S4 E-cadherin and microRNA levels in metaplastic and ductal tumours. **(a)** Representative photographs (taken at 40x and 200x) of the mesenchymal and the epithelial areas of a metaplastic breast cancer, from a histologic section stained with Haematoxylin and Eosin (H&E), with corresponding results of immunohistochemistry using cytokeratin (CK) and E-cadherin. In this specimen, discrete mesenchymal (sarcomatoid) and epithelial (epithelioid) regions were observed. The epithelioid region expressed E-cadherin and retained epithelial features, whereas the sarcomatoid region displayed a spindle shaped morphology and lacked

E-cadherin. Despite the morphologic heterogeneity of metaplastic carcinoma, cytokeratin is often expressed in both the epithelioid and sarcomatoid regions, as in the example above, implying they are derived from epithelial origin. In addition, the patterns of metastasis of metaplastic tumours are similar to those of the more common types of breast cancer, so that for diagnostic and therapeutic purposes this tumour is regarded as a form of breast carcinoma, rather than a sarcoma. **(b)** Relationship between E-cadherin and microRNA levels in ductal and metaplastic tumours. Ductal tumours are coloured in blue and metaplastic in red. Pearson correlation coefficients are shown.

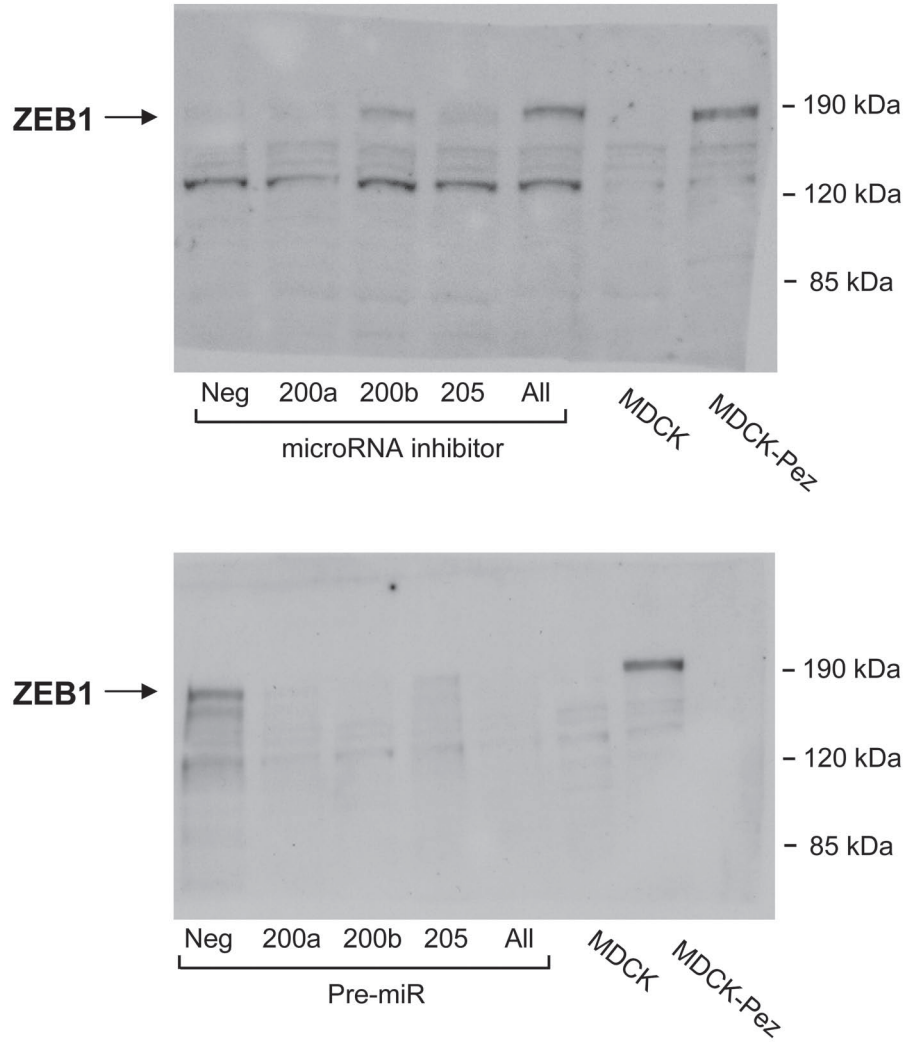


Figure S5 Full scan images of immunoblots shown in Figure 4. Membranes were cut according to the pre-stained molecular weight markers and probed with a ZEB1-specific antibody.

Table S1 Oligonucleotides used in real-time PCR, cloning, and knockdown studies. Primers are labelled by gene name, species (where appropriate) and direction (5' = for, 3' = rev). miRNA knockdown RNAs are 2'-O-methyl modified. Primers used for mutating the miR-200b seed regions in the ZEB1 and SIP1 3'UTRs are numbered according to their position from 5' to 3' with mutated bases marked in bold.

Table S1 Oligonucleotides used in real-time PCR, cloning, and knockdown studies

Primer Name	Sequence (5' to 3')
Real time PCR	
ZEB1 hum-dog for	TTCAAACCCATAGTGGTTGCT
ZEB1 hum-dog rev	TGGGAGATACCAAACCAACTG
SIP1 hum for	CAAGAGGCGCAAACAAGC
SIP1 hum rev	GGTTGGCAATACCGTCATCC
SIP1 dog for	CGGTCCAGAAGAAATGAAGG
SIP1 dog rev	TCCTCAAAGTCTGATGTGCAA
E-cadherin hum for	CCCACCACGTACAAGGGTC
E-cadherin hum rev	CTGGGGTATTGGGGGCATC
E-cadherin dog for	AAGCGGCTCTACAACCTCA
E-cadherin dog rev	AACTGGGAAATGTGAGCACC
N-cadherin dog for	CAACTTGCCAGAAAACCTCCAGG
N-cadherin dog rev	ATGAAAACCGGGCTATCAGCTC
Fibronectin dog for	GCAACTCTGTGGACCAAGG
Fibronectin dog rev	CACTGGCACGAGAGCTTAAA
GAPDH hum for	ACCCAGAAGACTGTGGATGG
GAPDH dog for	CATCACTGCCACCCAGAAG
GAPDH hum-dog rev	CAGTGAGCTTCCCGTTCAG
ZEB1/SIP1 3'UTR cloning	
ZEB1 3'UTR for	CAACTAGTCAAAAATAAAATCCGGGTGTGC
ZEB1 3'UTR rev	TTACTAGTACAGCAGTTCAGGCTTGTGTA
SIP1 3'UTR for	ATACTAGTGGAGTTGGAGCTGGGTATTG
SIP1 3'UTR rev	ACACTAGTTGGAATCAGGATCAGTTGAGAA
ZEB1/SIP1 3'UTR mutagenesis	
ZEB1 miR-200b site 1 for	GCATCTGGCATTGTTTTATCTTATCAGGACTATCACTCTTATGTTGGTTTATTCTTA
ZEB1 miR-200b site 1 rev	CGTAGACCGTAACAAAATAGAATAGTCCTGATAGTGAGAATACAACCAAATAAGAAT
ZEB1 miR-200b site 2 for	ATTGGTAAACATA TGCTAAATCCGCCTCAGGACTTTATTATGTTTTTAAAAATGTGAGAACTT
ZEB1 miR-200b site 2 rev	TAACCATTTGTATACGATTTAGGGCAAGTCTGAAATAATACAAAAAATTTTACTCTTGAA
ZEB1 miR-200b site 3 for	TGTAAGTGCCATTCTCAGGACTTTCAAGGCTCTAACCCGC
ZEB1 miR-200b site 3 rev	ACATTCACGGTAAAGAGTCTGAAAGTTCGAGATTGGGCG
ZEB1 miR-200b site 4 for	ATTAACAACATTAGCTGATTTTACCTATCAGGACTATTTTATTTCTTTAGTTTATAGATCTGTGC
ZEB1 miR-200b site 4 rev	TAATTGTTGTAATCGACTAAAAATGGATAGTCTGATAAAAAATAAGAAAAATCAAATATCTAGACACG
ZEB1 miR-200b site 5 for	CTGTATGTCTTCAAACCTGGCAGGACTAATACCCCTTCTACTGACATAT
ZEB1 miR-200b site 5 rev	GACATACAGAAGTTTGGACCGTCTGATTATGGGAAGAATGACTGTATA
SIP1 miR-200b site 1 for	GGTGCCCGCACTACCATAACATCAGGACTTTTATTATTATTATTGTTATTCTCT
SIP1 miR-200b site 1 rev	CCACGGGCGTGATGGTATGTAGTCTGAAAAATAATAATAATAACAATAAGGA
SIP1 miR-200b site 2 for	GCTCGCACTACAATGCATCAGGACTAATGATTCCTCTGTACTTTCC
SIP1 miR-200b site 2 rev	CGAGCGTGATGTTACGTAGTCTGATACTAAGGAGACATGAAAGG
SIP1 miR-200b site 3 for	CTTTGAAGCACCCATGTCAGCAGTAGAAGAATAGGCAGCAGTT
SIP1 miR-200b site 3 rev	GAAACTTCGTGGGTACAGTCTGCTATCTTCTTATCCGTCGTC
SIP1 miR-200b site 4 for	CTGTACTTTTTGTTCAATTAATTTTGTGACAGTACACCAAACCTGTTTTGCAACAAAAAAT
SIP1 miR-200b site 4 rev	GACATGAAAAACAAGTAATTAATAAACAGTCTGTCATGTGGTTTGACAAAAACGTTGTTTTTTTA
SIP1 miR-200b site 5 for	TATTTCCCTAATTTTATTATTTCATACTGTAGTGTACAGCAGTATAGTCTTCAATATATAGATATATTTTAGTAAAAAAG
SIP1 miR-200b site 5 rev	ATAAAGGATTAATAATAATAAAGTATGACATCACATGTCGTCATATCAAGAAGTTATATATCTATATAAAAAATCATTTTTTC
SIP1 miR-200b site 6 for	ATGACAAAAATCTTTCTCAATTTGCTTTGTAAGGACTATTGAAATTTCAATTTGTAATTTCTTTTGAAAAATG
SIP1 miR-200b site 6 rev	TACTGTTTTTAGAAAAGGCTAACAGAAAAACATTTTCTGATAACTTAAAAAGTTAAACATTAAGAAAAAATTTTAC
miR-200 family cluster cloning	
miR-200b-200a-429 for	AGAATTCCTACTCCGACCTAGTCTCTC
miR-200b-200a-429 rev	AACCTAGGCTCCGGGTATCTGTGACTGTGAC
miR-200c-141 for	AGAATTCAGGGCTCACCAGGAAGTGT
miR-200c-141 rev	GTCCTAGGAGGGGTGAAGGTCAGAGGTT
miRNA knockdown	
2'-O-methyl miR-200a	UUGAACAUUGUACCAGACAGUGUUAGAGUC
2'-O-methyl miR-200b	CGCCGUAUCAUACCAGGCGAUUUAGAGA
2'-O-methyl miR-205	AUAGUCAGACUCCGGUGGAAUGAAGGACGAU
2'-O-methyl control	CAUCACGUACGCGGAUACUUCGAAAAUGACC
ZEB1 and SIP1 knockdown	
ZEB1-A siRNA	GCCAACAGUUGGUUUGGUATT
ZEB1-B siRNA	GCAUCCAAAGAACAAGAAATT
SIP1-A siRNA	CCUCUUGUCAUCUGUACUUTT
SIP1-B siRNA	GCAUGUAUGCAUGUGACUUTT